Intact finger representation within primary sensorimotor cortex of musician's dystonia

Anna Sadnicka,[1,2] Tobias Wiestler,[2] Katherine Butler,[3,4,5] Eckart Altenmüller,[6] Mark J. Edwards,[1] Naveed Ejaz[7] and Jörn Diedrichsen[7]

Abstract

Musician's dystonia presents with a persistent deterioration of motor control during musical performance. A predominant hypothesis has been that this is underpinned by maladaptive neural changes to the somatotopic organisation of finger representations within primary somatosensory cortex. Here, we tested this hypothesis by investigating the finger-specific activity patterns in the primary somatosensory and motor cortex using functional MRI and multivariate pattern analysis in nine musicians with dystonia and nine healthy musicians. A purpose-built keyboard device allowed characterisation of activity patterns elicited during passive extension and active finger presses of individual fingers. We analysed the data using both traditional spatial analysis and state-of-the art multivariate analyses. Our analysis reveals that digit representations in musicians were poorly captured by spatial analyses. An optimised spatial metric found clear somatotopy but no difference in the spatial geometry between fingers with dystonia. Representational similarity analysis was confirmed as a more reliable technique than all spatial metrics evaluated. Significantly, the dissimilarity architecture was equivalent for musicians with and without dystonia. No expansion or spatial shift of digit representation maps were found in the symptomatic group. Our results therefore suggest that the neural representation of generic finger maps in primary sensorimotor cortex is intact in musician's dystonia. These results speak against the idea that task-specific dystonia is associated with a distorted hand somatotopy and lend weight to an alternative hypothesis that task-specific dystonia is due to a higher order disruption of skill encoding. Such a formulation can better explain the task-specific deficit and offers alternative inroads for therapeutic interventions.

Author affiliations:

1 Movement Disorders and Neuromodulation Group, St. George's University of London, UK

2 Department of Clinical and Movement Neurosciences, University College London, UK

3 Faculty of Health, School of Health Professions, University of Plymouth, UK

4 Division of Surgery and Interventional Science, University College London, UK

5 London Hand Therapy, King Edward VII's Hospital, UK

6 Hannover University of Music, Drama and Media, Germany.

7 Western Institute of Neuroscience, University of Western Ontario, Canada

Correspondence to: Anna Sadnicka

Movement Disorders and Neuromodulation Group, St. George's University of London, SW17 0RE, UK

E-mail: asadnick@sgul.ac.uk

Running title: Finger representation in musician's dystonia

Keywords: task-specific dystonia; focal hand dystonia; primary somatosensory cortex; primary motor cortex; representation, homunculus

Introduction

Task-specific dystonia is a form of isolated dystonia that presents with a selective motor impairment during the performance of a specific skill.[1] For example, in musician's dystonia there is normal use of the fingers for writing or typing yet the individual is *unable* to fluently co-ordinate the same fingers during musical performance.[2] The highest relative prevalence of task-

specific dystonia is seen within professional musicians with 1- 2% affected.[1] For many this is the end of performance careers, with a devastating impact for both the individual and their contribution to our cultural society.[3]

A highly influential animal model of task-specific dystonia has dominated research over the last two decades.[4] In this model, two monkeys were trained to perform rapid, repetitive, highly stereotypic grasping movements until a painful forearm syndrome developed and motor performance deteriorated significantly.[4] Subsequent electrophysiological mapping of the representations of the hand within primary somatosensory cortex (S1) revealed a 10-20 fold increase in the size of the sensory receptive fields of neurons. In addition, there was the breakdown of normally segregated areas, for example, the representation of the dorsal and palmar aspects of hand were found to be overlapping. Motivated by this primate study, electrophysiological and imaging studies in humans have also provided evidence of distorted finger representations within S1 in task-specific dystonia.[5-11] Therefore, one hypothesis is that the pathophysiology of task-specific dystonia is caused by a distorted somatotopy of the hand in S1.

However, alternative disease models have been proposed as altered representations within primary cortical regions are unable to explain many clinical features. For example, such a model cannot explain task-specificity. Abnormal digit representations in S1 would predict a general deficit of *any* task in the implicated fingers as the representation or encoding of sensory information at its lowest level is corrupted. Additionally, even within the affected task, dystonia is varied in its manifestations. Some musicians only experience deficits only within a particular sequence with precise spatial and temporal features (such as playing tremolo on the guitar, or an ascending scale rather than a descending scale on the piano). Such features represent complex and more abstract features of movement that are encoded within higher order control regions of the sensorimotor hierarchy such as the premotor and parietal cortices.[12]

Significantly, recent advances in the analysis of distributed brain activity patterns have substantially updated views of how the hand and fingers are represented in sensorimotor cortex.[13] Traditional approaches stressed the orderly spatial mapping of body parts to different regions of the brain, reinforcing the notion of the iconic homunculus. Yet, functional MRI (fMRI) studies in healthy individuals show substantial overlap between cortical areas activated by different body

parts. Complex layouts are usually found with multiple peaks of activation in S1 and primary motor cortex (M1) and such patterns are highly variable across individuals[14,15]. This contrasts with the notion of a discrete, orderly layout for the hand with a segregated ordering of finger activity patterns as suggested by historical depictions of the homunculus. Recently, novel multivariate analysis methods (such as representational similarity analysis) have shown that although the actual spatial layout is variable across individuals, the relative overlap between specific finger pairs, as measured by the statistical pattern similarity, is highly preserved. This invariant organisation, with the thumb having the most unique representation and being most distinct from the ring finger, can be explained by the statistics of finger movements in everyday activities.[14] Thus, it appears that representations in sensorimotor cortex, rather than being dictated by a fixed spatial layout, arise from a mapping process of every-day actions onto the surface of the neocortex.[16]

We reasoned that, if an altered finger map in S1 is indeed the core neural correlate of task-specific dystonia, we should be able to detect a deviation from the normal, invariant organisation revealed by modern pattern analysis approaches. To test this idea, we characterised the finger representations in S1 and M1 using fMRI while individual fingers were either lifted passively or active pressing a custom-built piano-like device. We compared musicians with task-specific dystonia to healthy musicians using both conventional spatial measures, as well as pattern analysis approaches (Table 1). If the map of finger representations is altered in dystonia, then we should observe differences in the similarity structure of the underlying patterns. Specifically, the idea of increasing overlap and fusion of finger representations predicts a decreasing dissimilarity of the patterns of the affected fingers in musician's dystonia. Alternatively, a preserved organisation of basic finger representation in S1 and M1 would suggest that task-specific dystonia has alternative neural correlates.

Materials and methods

Participants

A total of 20 right-handed professional musicians took part in the study. All musicians fulfilled the following inclusion criteria: 1) had completed postgraduate musical training; 2) performed either as a soloist or ensemble player; 3) musicianship was their primary source of income. The patient group consisted of 11 musicians (10 male; mean age=49.9 years, SD=7.85). Patients were recruited via clinics at the National Hospital for Neurology and Neurosurgery and London Hand Therapy. Two neurologists (MJE and AS) with a special interest in musician's dystonia independently confirmed the diagnosis. For each patient, symptomatic fingers during musical performance with their primary instrument of choice were noted (guitar or piano). Symptomatic fingers were defined as (1) reported to be affected by patients and (2) had an objective deficit of motor control on examination by specialist (such as an abnormal posture, or recurrent pattern of abnormal movement on action). All patients had dystonic symptoms in the right-hand whist playing, two patients had bimanual symptoms (Table 2). The severity of overall impairment for each individual was quantified using the Tubiana and Chamagne scale.[17] The control group consisted of nine healthy musicians with no history of musculoskeletal/functional impairment of the upper limbs (all male; mean age=41.0 years, SD=14.5). The recruited group were approximately matched for age ($t(18)=-1.75$, $p=0.09$). The local ethics committee approved all study procedures and written consent was obtained from each participant according to the Declaration of Helsinki.

Experimental Design

Patients and controls attended two independent study sessions (i) consent, explanation and practice (ii) performance of task in the MRI scanner. Two patients were unable to complete the task in the fMRI scanner due to anxiety/claustrophobia and imaging data acquisition could not be completed. Equipment failure also resulted in failure of data collection for one control. In total data from nine musicians with dystonia and eight healthy musicians were analysed. While the final cohorts were matched for their musical expertise, the control group was on average slightly

younger (t(15) = -2.17, p=0.046). Unless otherwise stated, the significance level was $p<0.05$ for all comparisons.

fMRI procedure

Data were acquired on a Siemens 3T TRIO MRI scanner with a 32-channel head coil. For each participant, we measured the blood-oxygen-level dependent (BOLD) responses for passive and active movement conditions. We developed an fMRI compatible device with five piano-style keys (Figure 1). Each key had a small grooved circular platform for the fingertip. In the *passive* condition the circular platform was raised by a pneumatic piston so that the individual fingers of the right hand were passively extended by ~15mm (Figure 1, for details see[18]). This passive movement condition has no behavioural confounds (as patients can show increased co-contraction between fingers on individuated finger presses). The pistons/passive condition were a feature of the right-hand box only. During the *active* movement condition, participants performed individuated finger presses using right and left-hand boxes and finger forces were recorded.

The experiment began with participants fixating on a star in the centre of the screen. At the start of each trial, during a 1.36s instruction period, the fixation star turned a different colour to indicate one of three experimental conditions: 1) red indicated the passive condition, 2) green indicated the active condition and 3) white indicated a rest condition. Trials lasted 10.54s and consisted of the instruction period, a 9s period in which the six responses / passive lifts were made and a short inter-trial-interval (180ms). During the *passive/lift* condition, the red star persisted, and a keyboard outline indicated which finger would be lifted six times (for 1s, with a 0.5s break before the next lift). For the *active/press* condition the instructed finger was highlighted in green on a keyboard outline. During the response period the star was replaced with a green letter 'p', which was the go-cue for participants to make a short isometric force press with the instructed finger. A force of 2.3N was required to register a successful key press following which the letter ‘p’ disappeared. The letter 'p' reappeared again after 1.5s to signal the start of the next press with six key presses in total. Instructed fingers for each trial were selected in a pseudo-random order, such that all possible combinations were tested twice in each run (ten

active press conditions (two hands, five fingers) and five passive conditions for the fingers of the right hand only). During the *rest* condition participants were instructed to relax fingers maintaining contact with the keyboard in both hands. There were 3-5 rest conditions of varying lengths (14.9s, 25.5s or 36.1s) that were randomly interspersed within each run.

Eight functional runs were collected in total and in each 126 images were obtained at an in-plane resolution of 2.3mm x 2.3mm (2D echo-planar sequence, TR=2.72s, 32 interleave slices with thickness=2.15mm and gap=0.15mm, matrix size=96x96). The first three images in the sequence were discarded to allow magnetisation to reach equilibrium. Field maps were obtained and used to correct for field strength inhomogeneities[19]. Finally, a T1-weighted anatomical scan was obtained (3D gradient echo sequence, 1 mm isotropic, field of view=240 × 256 × 176mm).

Imaging analysis

The functional imaging data from each participant was minimally pre-processed using SPM tools[20]. The data were corrected for slice timing and were corrected for head motion across by aligning all functional images to the beginning of the first run (three translations: x, y, z and three rotations: pitch, roll, yaw). Functional data were then co-registered to each participants' T1-image. No spatial smoothing or spatial normalization to a group template was applied at this point. The time-series data at each voxel were high-pass filtered with a cut-off frequency of 128s. The pre-processed functional data was then analysed using a generalised linear model, with a separate regressor for each trial condition/finger/run. Each condition was modelled using a boxcar function which covered the duration of the six stimulations or presses (duration=9s as detailed above). Boxcar functions were convolved with a standard hemodynamic response function. To control for movement-related artefacts, we used the robust-weight-least square toolbox in SPM.[21]

The parameter estimates for each run and condition was divided by the root mean-square error from the first level model to obtain a t-value for the condition>rest contrast. These t-values were then used to investigate the organisation of finger maps in S1 and M1. Each participant's T1-image was used to reconstruct the pial and white-grey matter surfaces using Freesurfer.[22] The surfaces are meshes that consist of nodes that are connected with edges. Individual surfaces were inflated to a sphere and then registered across participants by matching them to a common

template (fsaverage) using the sulcal-depth map and local curvature as minimisation criteria. Two regions of interest (ROIs) were defined on the group surface using probabilistic cyto-architectonic maps aligned to the average surface.[23] Surface nodes with the highest probability for Brodmann area (BA) 4 1.5cm above and below the hand-knob were selected as belonging to the hand area of M1. Similarly, nodes in the hand-region in BA 3a and 3b, again 1.5cm above and below the hand knob were selected for the hand area of S1. We did not consider BA 1 and 2, as finger representations tend to be more overlapping and less clearly organised even in healthy controls.[24] To avoid possible contamination of signals across the central sulcus, we excluded all voxels that had more than 25% of its volume located on the opposite side of the sulcus. All other voxel that were partly positioned in the between the pial and white-grey matter surface in the two ROIs were used in the analysis.

Quantifying finger representations using spatial analysis

Previous studies have reported that the spatial distances between different finger representations were significantly reduced in dystonia. Motivated by these studies, we employed different spatial and multivariate measures to characterise the activity pattern in S1 (BA3a and BA3b) and M1 (BA4) to determine whether patients showed an altered structure of finger representations relative to controls. We analysed the activity maps for passive and active finger movements on the right hand (symptomatic in musician's dystonia). The t-values for each finger were projected onto a flattened version of each individuals' surface. To analyse the spatial layout of the finger representation we employed a number of different methods to seek replication of previous studies. For the first method, we used the location of the maximal activity for each finger (see Figure 3) within the predefined ROI (see above). In the second approach, in order to take into account the entire activated region, we used the centre of gravity (COG) of the activation pattern, the average x and y location of each surface vertex, weighted with w_i.

$$\hat{x} = \sum_{i=1}^{P} x_i w_i \Big/ \sum_{i=1}^{P} w_i$$

$$\hat{y} = \sum_{i=1}^{P} y_i w_i \Big/ \sum_{i=1}^{P} w_i$$

In the case for the linearly-weighted COG, we set w_i to the t-value for positive activations, and to 0 for negative activations. We also tested other ways of calculating the COG: We used a activation contrast compared to the mean of all the fingers, and we explored introducing a statistical threshold before calculating the COGs. None of these variations led to a higher reliability than the original method.

Finally, to obtain different compromises between the maximal activation and the COG approach, we also calculated the COG, using a weighted softmax function[27] of the t-value (t_i) as w_i.

$$w_i = \frac{\exp(kt_i)}{\sum \exp(kt_i)}$$

For a softmax parameter *k=0*, all surface nodes would have the same weight and the resultant coordinate would be the COG of the entire ROI. For larger value of k, the weight of the more highly activated surface nodes will be much higher than for the other nodes. In the extreme of $k \to \infty$, the coordinate will simply reflect the location of the maximal activation. Thus, by varying *k* over multiple values (0.05, 0.1, 0.2, 0.4, 0.8, 1.6, 3.2) we were able to explore analyses that either took into account the entire activated area or concentrated on the areas of highest activation (see Figure 4).

To assess for a systematic somatotopic ordering of the finger representation across participants, we performed a repeated-measures MANOVA for each group, using the x- and y- coordinates for each finger as dependent measures, and the digit as an independent variable. The MANOVA test for any systematic differences between the spatial locations of any pair of finger across participants.

To test group differences in the spatial layout of digit representations, we calculated the Euclidian distance on a flattened representation on the cortical surface between the 10 possible pairs of digits. We then compared the average distance between groups using a Student *t*-test for independent samples. We also assessed for differences in the relative spatial layout by submitting the 10 distances to a repeated measures ANOVA and assessing the group x digit pair interaction using an *F*-test.

Quantifying finger representations using representational similarity analysis

As an alternative to spatial measures of finger representations, we also employed representational similarity analysis (RSA), which assesses the similarity between different activity patterns in the ROI, while ignoring the spatial arrangement.[25,26] The beta-weights from the generalised linear model were extracted to obtain the finger-specific activity patterns in the ROIs. The dissimilarity between the activation patterns for each finger pair (z_i, z_j) was computed using the cross-validated Mahalanobis distance.[27] The voxel-by-voxel covariance matrix Σ was estimated from the residual from the first-level model and regularised by shrinking all off-diagonal elements towards zero.[28] An unbiased estimate for the squared Mahalanobis distance can then be calculated as:

$$d_{i,j}^2 = \frac{1}{M}\sum_{m=1}^{M}\left(z_i - z_j\right)_m^T \Sigma^{-1}\left(z_i - z_j\right)_{\sim m}$$

For each of the M runs, the patterns are estimated from the data from that run (m) or from all other runs (~m). This cross-validation procedure ensures that the expected value of *d* is zero if two patterns are not different from each other and that the distance estimates are unbiased.[32] We computed distances between all 10 pairwise combinations of fingers, separately for each active/passive movement condition, for each hand, and within each ROI (S1 and M1). Statistical group differences in the average distance and relative arrangement were tested as described for the spatial distances. The relative arrangement of the digits can also be visualised in a two-dimensional representational space using classical multi-dimensional scaling.[33]

Split half reliability

To quantify the reliability of the different methods we determined the split-half reliability of the 10 pairwise distances between digit centres, using odd and even runs from each participant. Both the spatial distances and RSA dissimilarity were calculated on the 4 runs in each half, and the reliability was calculated as the correlation of the distance vector for all finger pairs across odd and even runs.

Surface-based searchlight analysis

To detect possible overall differences in the location or spatial extent of the digit representation, we also conducted a searchlight analysis.[29] Based on the individual cortical surface reconstruction, we selected - for each surface node - a circle on the surface that contained 60 voxels between the pial and the white-matter surface. For each of these searchlights, we computed the average cross-validated Mahalanobis distance across all 10 pairs of fingers (see above). The average dissimilarity was then mapped back to the node in the centre of the searchlight. By repeating this process for each surface node, we build up a cortical map of cortical regions that contained digit information for each participant. The maps were then compared using a *t*-test for independent samples and uncorrected threshold of t_{15}= 3.2860, p<0.005, and corrected for cluster size using Gaussian Field map correction.[30]

Data availability

Summary data and analysis code are available online at github.com/nejaz1/project_dystonia.

Results

We wanted to determine whether there were measurable alterations of finger representations in the primary sensorimotor cortices in musician's dystonia. We therefore used fMRI to measure evoked-BOLD responses in S1 and M1 during passive finger lifts and active finger presses in our cohort of participants. For the main analysis we focused on the passive condition, as it allows for the unbiased assessment of finger representations independent of possible behavioural differences (see methods). All results, however, were also replicated in the active condition.

As expected, the activity patterns for each finger lift were distributed with substantial overlap between the different fingers in both pre- and post-central gyrus, even in healthy musicians (Figure 2). Furthermore, there was a substantial variability in finger-specific activity patterns across individuals.[14] Motivated by previous papers, we initially considered spatial measures to characterise the digit representations in S1 and M1. Given that there are a large number of possible methods to summarize the spatial layout of digit representations, we took a two-step

approach. We first considered a range of different methods and compared them in terms of their reliability. We then used to the most reliable method only to test for control-patient differences.

To determine the location of the representation of each finger, we used either the location of maximal activation (Figure 3A, star) or the centre of gravity of the activated vertices, weighted by the size of the activation (Figure 3A, cross). To explore a wider range of intermediate methods, we applied a softmax approach (see method). By varying the softmax parameter k, we can weight each positively activated vertices equally (k=0), or only use the most highly activated vertex ($k \to \infty$,). As can be seen in Figure 3A, the variation allows a trade-off between taking into account the entire activated regions and concentrating only on the most active regions. The Euclidean distances between the five estimates for the different fingers gave 10 pairwise distances, which in turn quantified the spatial geometry of finger representations in the hand-knob for each individual.

To decide between these different methods of characterising the spatial layout, we determined the split-half reliability of the 10 pairwise distances between digit centres, using odd and even runs from each participant. Both the COG method, as well as the point of maximum activation led only to a mediocre within-subject reliability, with split-half correlations around 0.4 for S1 and 0.3 for M1. The softmax approach performed best, with a value of k=0.8 providing a best compromise between the entire region of activation and the most highly activated regions. For all subsequent spatial analyses, we focused therefore on this metric.

Within each group, the softmax COG estimates were sensitive and reliable enough to uncover a clear somatotopic order of finger representations in S1. A repeated-measures MANOVA across fingers was significant for healthy musicians (χ^2_7=34.82, p=2.879e-05), as well as for musicians with dystonia (χ^2_8= 23.28, p= 0.0037). Using this metric, however, we found no differences in the average spatial distances between digit centres (S1: t_{15}=0.070, p=0.945, M1: t_{15}=0.427, p=0.676). We also did not detect any change in the pattern across the 10 individual inter-digit distances (S1: $F_{9,135}$=1.0864, p=0.3769; M1: $F_{15,135}$=0.8003, p= 0.6166). Taken altogether, the extent and exact geometry of somatotopic ordering of finger representations was indistinguishable between musicians with and without dystonia.

Spatial measures to quantify finger representations have significant weaknesses. Consider for example the activity patter for the index finger shown in the first row of Figure 2 which shows

four different small cluster of activity in S1. Any spatial measure summarises these clusters into one location, therefore providing only a poor description of the complexity of the underlying map.

To overcome this limitation of spatial metrics, in our second analysis we used multivariate pattern analysis to quantify finger representations. We estimated the cross-validated Mahalanobis distances (see methods) between all pairs of evoked-activity patterns during passive stimulation of the fingers in the right hand. The split-half reliabilities for RSA measures were above 0.8, significantly higher in both S1 and M1 than any of the spatial measures (Figure 3B). Using the reliable RSA measure of the overlap of the finger-specific activity patterns, we did not find a significant difference between the groups: In S1, the average dissimilarity was 0.521 (standard error: ±0.048) for the controls, and 0.510 (±0.037) for the patients, t_{15}=0.185, p=0.855. Similarly, we did not find a difference in M1 (controls: 0.506±0.056, patients: 0.515±0.049, t_{15}=-0.122, p=0.905).

These null-results, however, need to be considered in light of the relatively small sample size in our study. To assess how much evidence, we had for the equivalence of inter-digit distances in patients and controls, we computed the Bayes Factor between the null hypothesis (no difference) and the alternative hypothesis. In the absence of a good reference from clinical studies in dystonia for the expected effect size, we used a recent study in normal controls, which investigated the influence of a temporary digital nerve block.[31] This study used identical imaging and analysis methods. The passive task (full details[32]) resulted in a 29% reduction of the average inter-digit dissimilarity. If we evaluate the observed *reduction* in average inter-digit dissimilarity seen in patients relative to controls in S1 (-2.11%) under the null model of no reduction (H0) and under the alternative hypothesis of a 29% reduction we find that the Bayes Factor in favour of the null hypothesis (BF_{01}) of 10.91. This suggests that the result is ~11 times more likely under the null as compared to the alternative hypothesis which is usually considered to be strong evidence in favour of the null hypothesis.[33] For M1, that Bayes factor was BF_{01} = 7.83 in favor of the Null-Hypothesis of no difference, again providing strong evidence for the absence of a difference between controls and patients.

We then investigated whether there were any changes in the relative structure of the dissimilarities between controls and patients, which can be visualised by plotting the normalized

dissimilarities across all digit pairs (Figure 5A-B), or in two dimensions using multidimensional scaling (Figure 5C). Replicating earlier studies[14], we found that this structure was highly *invariant* across subjects, with the largest dissimilarities for thumb and ring fingers and smallest for the middle and ring fingers. Importantly, we did not find any group difference in the pattern of dissimilarities (S1: $F_{9,135}$=0.26, p=0.9831, M1: $F_{9,135}$=0.03, p=0.999). We also tested for a difference between the distances involving the affected fingers compared to the non-affected fingers in the dystonic group. We did not find a significant difference, (S1: t_8=-1.672, p=0.133, M1: t_8=-0.504, p=0.627), and if anything, the distances involving affected fingers were larger than those only involving unaffected fingers, contrary to the idea dystonia is associated with a loss of separation between cortical digit representation.

We also asked whether we could detect any expansion or spatial shift of the entire digit representation across the sensorimotor cortex. Figure 5E shows a surface-based searchlight map of places on the lateral hemisphere, were the local activity patterns differed between different fingers. For both healthy control musicians and musicians with dystonia, the hand area of M1 and S1 are clearly visible. A statistical comparison between the two maps (see methods), did not yield any significant clusters of increase or decrease distances in the patient group.

Finally, all reported results were also replicated in the active condition, in which the participants made isolated finger presses with their right (affected) hand (Figure 5F-G). We did not find any difference in the average dissimilarity (S1: t_{15}=-0.636, p=0.534, M1: t_{15}=-0.765, p=0.456), nor did we detect and differences in the pattern architecture across all digit pairs (S1: $F_{9,135}$=0.56, p=0.825, M1: $F_{9,135}$=0.32, p=0.968). As for the passive condition, we conducted a Bayesian analysis, this time against an observed 19% reduction of the average inter-digit dissimilarity[31] for the active condition. Again, we found clear evidence that there was no difference between patients and controls in the average inter-digit distance (S1: BF_{01}=7.41, M1: BF_{01}=4.17).

To summarise, even when using an optimised measure of pattern organisation, we were unable to detect any alteration of basic finger representations in primary sensorimotor cortex between musicians with and without dystonia. Neither the overall location nor extent of the digit representation (Figure 5E), nor the arrangement of the digit-specific patterns within this region (Figure 5A-D, F-G), showed any group difference. Overall, our results contradict previous

reports that argue that abnormal finger representations in primary sensorimotor cortex are the cause for the loss of finger control in musicians with dystonia.

Discussion

In this study, despite careful technical work, our fMRI data did not provide any evidence for an alteration or distortion of finger representations in S1 or M1 challenging the hypothesis that task-specific dystonia is caused by a distorted somatotopic organisation of fingers. We offer the alternative hypothesis that task-specific dystonia is encoded within a hierarchical skill network which has implications for how we design and prioritise future rehabilitation strategies.

The original evidence for somatotopic disruption in task-specific dystonia came from work in primates required to perform repetitive hand movements (Figure 6A).[34] One limitation of this experimental paradigm as a model for musician's dystonia is that monkeys were trained on repetitive whole hand grasping movements which are likely controlled differently from the fractionated movements of individual fingers akin to musical performance. Furthermore, from a conceptual point of view, it has always been difficult to define how abnormal S1 maps translate into a task-specific motor deficit. If the sensory representation of fingers were less differentiated in S1 for any finger, the corresponding blurring of incoming sensory data would presumably affect all manual tasks. Overall, therefore, it seems unlikely that causal neural engrams for dystonia are "hardwired" into generic hand maps within S1 (or M1).[35]

Methodologically, there are also limitations with experimental arguments used to support the somatotopic disruption model. In human studies, the overlapping nature and complexity of the activation patterns makes it difficult to find good metrics that summarise their spatial organisation. We have therefore systematically explored a range of methods that have been used in the literature. We found (in this work and previous studies) that the spatial metrics that span centre-of-gravity through to location-of-maximal-activation have low reliability within and across different healthy musicians. Since spatial metrics fail to reveal an invariant organisation of finger maps characteristic for a neurologically healthy individual it is over-optimistic to think that they should reveal systematic deviations from the healthy pattern in disorders such as task-specific dystonia. Representational similarity analysis, in contrast, was confirmed to uncover

representations that were highly robust within and between individuals.[14] Our passive finger lift condition focused on proprioceptive input and the active finger press corresponded to muscle activation patterns elicited during near isometric finger presses. However, despite the different behavioural features neither of these task conditions revealed changes in representational architecture.

These results therefore motivate the search for the neural correlates of task-specific dystonia away from generic digit maps in primary sensorimotor cortex. Such a stance fits with recent studies that have questioned whether spatial perceptual function is reliably impaired in focal dystonia.[36] Our data also reaffirms an expanding literature which emphasises that task-specific dystonia is a network disorder.[37-39] In health, the sensorimotor hierarchy involved in skill acquisition and performance is broad[40] and thus the breakdown of skill reproduction in task-specific dystonia may be due to distributed changes.[41] Intact motor control of fingers in alterative tasks suggests that *task-specific* representations and mechanisms should be sought[2,42]. Higher-order regions of the sensorimotor are likely to be involved. For example, intensive training of sequences of finger presses is associated with the stabilisation of *sequence* specific-activation patterns in premotor and parietal areas (whereas individual finger movements appear to be preferentially represented in M1 and S1, Figure 6).[18,43] An alternative lens is to also consider the feature space of risk factors and/or symptomatic abnormalities in task-specific dystonia.[35,41] For example, task-specific dystonia is seen more frequently in highly-trained skills such as musical performance. Experimentally it can be shown that highly-trained skills have extended planning horizons/sequences, a narrow capacity to generalise to other tasks and increasing automaticity.[44,45] These features contrast those seen with everyday skills and rely in distinct circuitries.[35,41,46-48]

Early retraining methods based on the distorted somatotopy hypothesis involved sensory super-training (such as learning braille), with the idea that improving sensory discrimination of the affected hand would lead to remapping and normalisation of dystonic digit maps within S1.[49-51] Our results provide a scientific rationale as to why sensory discrimination training does not appear to be reliably effective.[52] Our findings instead offer an optimistic therapeutic starting point as we believe that the neural representation of incoming sensory information related to passive lifts of individual fingers and the representation of the execution of individual finger

presses is intact. Therapeutic interventions that instead target the specific affected skill and its network are likely to have more yield. For example, disrupting engrained motor behaviours by reinjecting variability into movement repetitions has an emerging evidence base (e.g. sensorimotor retraining and differential learning).[35,53]

Of course, a limitation of our study is that our main conclusions rest on a null-result, that could also have been caused by insufficient sample size or insensitivity of fMRI to true alterations in the organisation of basic finger representations. However, the representational geometry demonstrates low inter-subject variability (Figure 5) and high intra-subject reliability (Figure 3) and a Bayesian analysis provides strong evidence for the equivalence of digit representations (at least if the expected reduction in inter-digit dissimilarities was similar to those reported using temporary digital nerve block[31]). Furthermore, we have carefully evaluated the different analysis methodologies previously used and found spatial metrics to be generally unreliable. Alternatively, we may have not captured neural differences due to the task tested. As discussed, it is likely that dystonia needs to be clinically manifest in order for the abnormal skill network to be activated. However, it is worth emphasising that none of the studies that reported altered somatic finger representations in the past used a task that generated dystonia. We therefore believe the identified shortfalls with the distorted somatotopy model are significant and valid.

In summary, this study found no evidence of abnormal finger representations in primary sensorimotor cortex using fMRI and multivariate pattern analysis. Our data support the development of alternative disease models involving a dysfunctional skill network that encodes the task-specific deficit of this disabling condition.

Acknowledgements

We thank the musicians with and without dystonia that generously gave their time for these experiments.

Funding

Anna Sadnicka was supported by a grant from the Guarantors of Brain as part of the Association of British Neurologists Clinical Research Training Fellowship Scheme and a Chadburn Clinical Lectureship in Medicine. Naveed Ejaz and Jörn Diedrichsen were supported by grants from the Wellcome trust (Grant 094874/Z/10/Z), and the Canada First Research Excellence Fund (BrainsCAN).

Competing interests

The authors declare no competing financial interests.

References

1 Altenmuller, E., Ioannou, C. I. & Lee, A. Apollo's curse: neurological causes of motor impairments in musicians. *Prog Brain Res* **217**, 89-106, doi:10.1016/bs.pbr.2014.11.022 (2015).

2 Hofmann, A., Grossbach, M., Baur, V., Hermsdorfer, J. & Altenmuller, E. Musician's dystonia is highly task specific: no strong evidence for everyday fine motor deficits in patients. *Med Probl Perform Art* **30**, 38-46, doi:10.21091/mppa.2015.1006 (2015).

3 Frucht, S. J. Focal task-specific dystonia in musicians. *Adv Neurol* **94**, 225-230 (2004).

4 Byl, N. N., Merzenich, M. M. & Jenkins, W. M. A primate genesis model of focal dystonia and repetitive strain injury: I. Learning-induced dedifferentiation of the representation of the hand in the primary somatosensory cortex in adult monkeys. *Neurology* **47**, 508-520, doi:10.1212/wnl.47.2.508 (1996).

5 Bara-Jimenez, W., Catalan, M. J., Hallett, M. & Gerloff, C. Abnormal somatosensory homunculus in dystonia of the hand. *Ann Neurol* **44**, 828-831, doi:10.1002/ana.410440520 (1998).

6 Elbert, T. *et al.* Alteration of digital representations in somatosensory cortex in focal hand dystonia. *Neuroreport* **9**, 3571-3575, doi:10.1097/00001756-199811160-00006 (1998).

7 Meunier, S. *et al.* Human brain mapping in dystonia reveals both endophenotypic traits and adaptive reorganization. *Ann Neurol* **50**, 521-527, doi:10.1002/ana.1234 (2001).

8 McKenzie, A. L., Nagarajan, S. S., Roberts, T. P., Merzenich, M. M. & Byl, N. N. Somatosensory representation of the digits and clinical performance in patients with focal hand dystonia. *Am J Phys Med Rehabil* **82**, 737-749, doi:10.1097/01.PHM.0000087458.32122.14 (2003).

9 Nelson, A. J., Blake, D. T. & Chen, R. Digit-specific aberrations in the primary somatosensory cortex in Writer's cramp. *Ann Neurol* **66**, 146-154, doi:10.1002/ana.21626 (2009).

10 Bleton, J. P. *et al.* Somatosensory cortical remodelling after rehabilitation and clinical benefit of in writer's cramp. *J Neurol Neurosurg Psychiatry* **82**, 574-577, doi:10.1136/jnnp.2009.192476 (2011).

11 Uehara, K. *et al.* Distinct roles of brain activity and somatotopic representation in pathophysiology of focal dystonia. *Hum Brain Mapp* **40**, 1738-1749, doi:10.1002/hbm.24486 (2019).
12 Kornysheva, K. & Diedrichsen, J. Human premotor areas parse sequences into their spatial and temporal features. *Elife* **3**, e03043, doi:10.7554/eLife.03043 (2014).
13 Kriegeskorte, N. & Diedrichsen, J. Peeling the Onion of Brain Representations. *Annu Rev Neurosci* **42**, 407-432, doi:10.1146/annurev-neuro-080317-061906 (2019).
14 Ejaz, N., Hamada, M. & Diedrichsen, J. Hand use predicts the structure of representations in sensorimotor cortex. *Nat Neurosci* **18**, 1034-1040, doi:10.1038/nn.4038 (2015).
15 Meier, J. D., Aflalo, T. N., Kastner, S. & Graziano, M. S. Complex organization of human primary motor cortex: a high-resolution fMRI study. *J Neurophysiol* **100**, 1800-1812, doi:10.1152/jn.90531.2008 (2008).
16 Graziano, M. S. & Aflalo, T. N. Mapping behavioral repertoire onto the cortex. *Neuron* **56**, 239-251, doi:10.1016/j.neuron.2007.09.013 (2007).
17 Tubiana, R. & Chamagne, P. [Occupational arm ailments in musicians]. *Bull Acad Natl Med* **177**, 203-212; discussion 212-206 (1993).
18 Berlot, E., Popp, N. J. & Diedrichsen, J. A critical re-evaluation of fMRI signatures of motor sequence learning. *Elife* **9**, doi:10.7554/eLife.55241 (2020).
19 Hutton, C. *et al.* Image distortion correction in fMRI: A quantitative evaluation. *Neuroimage* **16**, 217-240, doi:10.1006/nimg.2001.1054 (2002).
20 Penny, W., Friston, K., Ashburner, J., Keibel, S. & Michos, T. *Statistical Parametric Mapping: The Analysis of Functional Brain Images.* . 1 edn, (Academic Press, 2006).
21 Diedrichsen, J. & Shadmehr, R. Detecting and adjusting for artifacts in fMRI time series data. *Neuroimage* **27**, 624-634, doi:10.1016/j.neuroimage.2005.04.039 (2005).
22 Dale, A. M., Fischl, B. & Sereno, M. I. Cortical surface-based analysis. I. Segmentation and surface reconstruction. *Neuroimage* **9**, 179-194, doi:10.1006/nimg.1998.0395 (1999).
23 Fischl, B. *et al.* Cortical folding patterns and predicting cytoarchitecture. *Cereb Cortex* **18**, 1973-1980, doi:10.1093/cercor/bhm225 (2008).
24 Arbuckle, S. A., Pruszynski, J. A. & Diedrichsen, J. (bioRxiv, 2021).

25 Kriegeskorte, N., Mur, M. & Bandettini, P. Representational similarity analysis - connecting the branches of systems neuroscience. *Front Syst Neurosci* **2**, 4, doi:10.3389/neuro.06.004.2008 (2008).

26 Diedrichsen, J. & Kriegeskorte, N. Representational models: A common framework for understanding encoding, pattern-component, and representational-similarity analysis. *PLoS Comput Biol* **13**, e1005508, doi:10.1371/journal.pcbi.1005508 (2017).

27 Diedrichsen, J., Provost, S. & Zareamoghaddam. On the distribution of cross-validated Mahalanobis distances. (2016).

28 Ledoit, O. & Wolf, M. Improved estimation of the covariance matrix of stock returns with an application to portfolio selection. *J Empir Financ* **10**, 603-621 (2001).

29 Oosterhof, N. N., Wiestler, T., Downing, P. E. & Diedrichsen, J. A comparison of volume-based and surface-based multi-voxel pattern analysis. *Neuroimage* **56**, 593-600, doi:10.1016/j.neuroimage.2010.04.270 (2011).

30 Friston, K. J., Worsley, K. J., Frackowiak, R. S., Mazziotta, J. C. & Evans, A. C. Assessing the significance of focal activations using their spatial extent. *Hum Brain Mapp* **1**, 210-220, doi:10.1002/hbm.460010306 (1994).

31 Wesselink, D. B. *et al.* Malleability of the cortical hand map following a finger nerve block. *Sci Adv* **8**, eabk2393, doi:10.1126/sciadv.abk2393 (2022).

32 Sanders, Z. B., Wesselink, D. B., Dempsey-Jones, H. & Makin, T. R. *Similar somatotopy for active and passive digit representation in primary somatosensory cortex* (2019).

33 Kass, R. & Raftery, A. E. Bayes Factors. *Journal of the Americal Statistical Association* **90**, 22 (1995).

34 Byl, N. N. *et al.* A primate model for studying focal dystonia and repetitive strain injury: effects on the primary somatosensory cortex. *Phys Ther* **77**, 269-284, doi:10.1093/ptj/77.3.269 (1997).

35 Sadnicka, A. & Rosset-Llobet, J. A motor control model of task-specific dystonia and its rehabilitation. *Prog Brain Res* **249**, 269-283, doi:10.1016/bs.pbr.2019.04.011 (2019).

36 Mainka, T. *et al.* Intact Organization of Tactile Space Perception in Isolated Focal Dystonia. *Mov Disord* **36**, 1949-1955, doi:10.1002/mds.28607 (2021).

37 Hanekamp, S. & Simonyan, K. The large-scale structural connectome of task-specific focal dystonia. *Hum Brain Mapp* **41**, 3253-3265, doi:10.1002/hbm.25012 (2020).

38 Lungu, C. *et al.* Defining research priorities in dystonia. *Neurology* **94**, 526-537, doi:10.1212/WNL.0000000000009140 (2020).
39 Pirio Richardson, S. *et al.* Research Priorities in Limb and Task-Specific Dystonias. *Front Neurol* **8**, 170, doi:10.3389/fneur.2017.00170 (2017).
40 Diedrichsen, J. & Kornysheva, K. Motor skill learning between selection and execution. *Trends Cogn Sci* **19**, 227-233, doi:10.1016/j.tics.2015.02.003 (2015).
41 Sadnicka, A., Kornysheva, K., Rothwell, J. C. & Edwards, M. J. A unifying motor control framework for task-specific dystonia. *Nat Rev Neurol* **14**, 116-124, doi:10.1038/nrneurol.2017.146 (2018).
42 Sadnicka, A. & Kornysheva, K. What's in a Name? Conundrums Common to the Task-Specific Disorders. *Mov Disord Clin Pract* **5**, 573-574, doi:10.1002/mdc3.12684 (2018).
43 Yokoi, A. & Diedrichsen, J. Neural Organization of Hierarchical Motor Sequence Representations in the Human Neocortex. *Neuron* **103**, 1178-1190 e1177, doi:10.1016/j.neuron.2019.06.017 (2019).
44 Ramkumar, P. *et al.* Chunking as the result of an efficiency computation trade-off. *Nat Commun* **7**, 12176, doi:10.1038/ncomms12176 (2016).
45 Wu, Y. H., Truglio, T. S., Zatsiorsky, V. M. & Latash, M. L. Learning to combine high variability with high precision: lack of transfer to a different task. *J Mot Behav* **47**, 153-165, doi:10.1080/00222895.2014.961892 (2015).
46 Mizes, K. G. C., Lindsey, J., Escola, G. S. & Olveczky, B. *Similar striatal activity exerts different control over automatic and flexible motor sequences* (2022).
47 Leijnse, J. N., Hallett, M. & Sonneveld, G. J. A multifactorial conceptual model of peripheral neuromusculoskeletal predisposing factors in task-specific focal hand dystonia in musicians: etiologic and therapeutic implications. *Biol Cybern* **109**, 109-123, doi:10.1007/s00422-014-0631-5 (2015).
48 Altenmuller, E., Ioannou, C. I., Raab, M. & Lobinger, B. Apollo's curse: causes and cures of motor failures in musicians: a proposal for a new classification. *Adv Exp Med Biol* **826**, 161-178, doi:10.1007/978-1-4939-1338-1_11 (2014).
49 Zeuner, K. E. *et al.* Sensory training for patients with focal hand dystonia. *Ann Neurol* **51**, 593-598, doi:10.1002/ana.10174 (2002).

50 Zeuner, K. E. & Hallett, M. Sensory training as treatment for focal hand dystonia: a 1-year follow-up. *Mov Disord* **18**, 1044-1047, doi:10.1002/mds.10490 (2003).
51 Byl, N. N., Nagajaran, S. & McKenzie, A. L. Effect of sensory discrimination training on structure and function in patients with focal hand dystonia: a case series. *Arch Phys Med Rehabil* **84**, 1505-1514, doi:10.1016/s0003-9993(03)00276-4 (2003).
52 Butler, K., Sadnicka, A., Freeman, J. & Edwards, M. Sensory-motor rehabilitation therapy for task-specific focal hand dystonia: A feasibility study. Hand Therapy. 2018 2018;23 (2)(11). *Hand Therapy* **23** (2018).
53 Rosset-Llobet, J. & Fabregas, S. *Rehabilitation and Plasticity of Task-Specific Focal Hand Dystonia*. 256-260 (2018).

Figure legends

Figure 1 Equipment for experiment. (A) A custom-built keyboard had pneumatic pistons embedded within each key to lift each finger (passive condition) and force transducers to capture finger presses (active condition). **(B)** Schematic diagram of the internal anatomy of keyboard.

Figure 2 Individual activity patterns of finger representations in the left sensorimotor cortex during passive extension movements of fingers of the right hand. Each row shows the activity patterns from a single individual; two healthy musicians and two musicians with dystonia. Note the considerable variability of finger-specific activation patterns across participants.

Figure 3 Comparison of different methods to characterise the spatial layout of digit representations. (A) Activity pattern (t-values) for the thumb and index finger of a selected control participant for the passive condition over the region of interest S1. Star: the location of peak activation on each map (max). Cross: the centre of gravity (COG) of the activated regions, weighted by the t-values for each vertex. Circles: softmax-weighted COG, with a k-parameter of 0.05 (close to COG of the region) to 3.2 (close to max). **(B)** Split-half reliability of the distances between digit representations for COG, softmax-approach, peak activation (max), and representational similarity analysis (RSA) for S1 and M1.

Figure 4 Somatotopic ordering of finger representations in S1. Using the optimised softmax-weighted COG (k-parameter = 0.8) a somatotopic arrangement of fingers was demonstrated at the group level. Large white circles indicate group mean, and small colored circle the individual variability: thumb = red, index = orange, middle = green, ring = pale blue, little= dark blue. Locations are shown on the same flattened cut out of the cortical surface as used in Figure 2 and 3. The location of the central sulcus marked by a dotted line.

Figure 5 Representational structures for passive and active movements are not altered in musician's dystonia. (A) Cross-validated Mahalanobis distances between activity patterns for passive finger lifts for each finger pair for the control group shown with shaded standard error (S1). The dissimilarities for individual participants (normalized to the mean dissimilarity across finger pairs) are shown in thin green lines. Values close to zero indicate the patterns are similar, higher values indicate distinct patterns. **(B)** Cross-validated Mahalanobis distances between

activity patterns for passive finger lifts for the patient group. The structure of dissimilarities was highly similar for patients and controls. (**C**) The structure of dissimilarities for S1 can also be visualised by projecting it into a low-dimensional space using multidimensional scaling. **(D)** The dissimilarity structure is also highly similar for passive finger lifts in M1. (**E**) The extent and location of digit representations for healthy musicians (controls) and musicians with dystonia. The average dissimilarity between digit-specific activity patterns is shown on an inflated version of the lateral left hemisphere in two rectangular panels. The location of the premotor cortex (PMC), superior frontal sulcus (SFS), central sulcus (CS), postcentral sulcus (PoCS) and intra-parietal sulcus (IPS) are indicated by dotted lines. Gray scale in the background indicates cortical folding (dark = sulcus, light = gyrus). The approximate mapping of the rectangular panel to the left hemisphere is illustrated and the average dissimilarity value indicated by colour bar: low dissimilarity red, high dissimilarity yellow. (**F, G**) Pairwise cross-validated Mahalanobis distances between activity patterns for active finger presses in S1 and M1.

Figure 6 Disease models for task-specific dystonia. **(A)** Traditional distorted somatotopy hypothesis. The receptive field for each finger in S1 is drawn (thumb=red, index=orange, middle =green, ring=light blue, little=dark blue). In health, this idealised cartoon shows receptive fields as discrete areas. The corresponding signal across a strip of cortex cleanly maps to an individual finger. In task-specific dystonia overlapping and disorganised receptive fields lead to a mixing of signals and uncertainty of finger mapping. **(B)** Possible neural representation of a complex task. A small piece of music, which requires a series of finger presses of the right hand on a piano, may be represented in a hierarchical fashion with sequences and chunks (short stereotyped elements grouped 4-2-3 in this example) that then in turn activate the elementary movement components. **(C)** An alternative task such as a series of keyboard presses requires the same sequence of finger presses as the piano task. However, if the chunking converges on a different pattern (e.g. grouping of 3-3-3), immediately a different set of higher order control elements are required for typing the same sequence of finger presses. This is one potential neural mechanism for a task-specific deficit. **(D)** Recent fMRI work in normal controls shows that while single finger movements are represented in M1 and S1 (blue), chunks (pink) and sequences (orange) are represented in overlapping regions of premotor and parietal cortex[41].

1

2 **Table 1 Summary of analyses**

Question	Approach	Result	Figure
How well do spatial fMRI metrics characterise the finger representation in S1?	Split-half reliabilities for a range of different metric were compared	Digit representations are poorly captured by single spatial measures	Figs 2 and 3
Does the spatial geometry differ between healthy musicians and musicians with dystonia?	Euclidean distance between fingers using highest performing softmax COG were calculated for each individual.	Both groups showed clear somatotopy yet the spatial geometry was indistinguishable	Fig. 4
Does multivariate pattern analysis better quantify finger representations in S1?	Representation similarity analysis (RSA) assessed the similarity between activity patterns for different fingers.	Split-half reliabilities for RSA were highly reliable in S1 (>0.8) and more consistent than all spatial metrics evaluated	Fig. 3
Is the representation structure in S1 altered in musicians' dystonia?	Dissimilarity between each finger pair was computed using the cross-validated Mahalanobis distance.	Dissimilarity architecture equivalent for patient and controls in S1	Fig. 5
Are there overall differences in the location or spatial extent of digit representations?	Statistical comparison of surface-based searchlight maps	No significant expansion or spatial shift of digit representation maps found	Fig. 5

3

4

Table 2 Demographic and clinical details of final patient group

Name	Age	Gender	Instrument	Symptomatic digits	Duration	Severity
d01	39	Male	Piano	Right thumb	2	3
d02	49	Male	Piano	Right and left thumb	5	2
d04	49	Male	Piano	Right middle and ring finger; left thumb	7	3
d06	51	Male	Guitar	Right thumb and index finger	6	2
d07	51	Female	Guitar	Right index, middle and ring finger	3	2
d08	39	Male	Guitar	Right middle finger	2	3
d09	47	Male	Piano	Right ring and little finger	4	4
d10	51	Male	Guitar	Right middle and ring finger	6	3
d11	49	Male	Guitar	Right thumb	16	2

Mean duration of dystonic symptoms was 5.66 years (SD=4.27). All patients had symptoms in the right-hand and two also had dystonia of the left thumb. The Tubiana-Chamagne scale (TCS) has the following possible values: 0 = unable to play; 1 = plays several notes but stops because of blockage or lack of facility; 2 = plays short sequences without rapidity and with unsteady fingering; 3 = plays easy pieces but is unable to perform more technically challenging pieces; 4 = plays almost normally, difficult passages are avoided for fear of motor problems; 5 = returns to concert performances). The average Tubiana-Chamagne score for the complete cohort was 2.66 (SD=0.701).

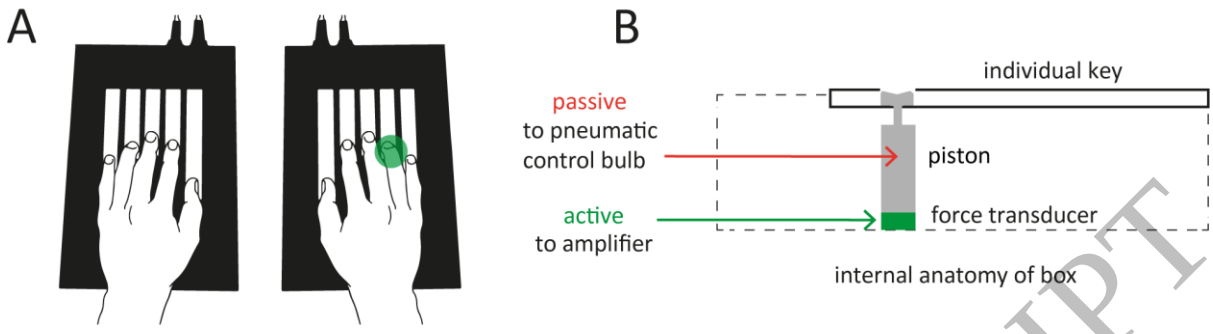

Figure 1
159x44 mm (5.2 x DPI)

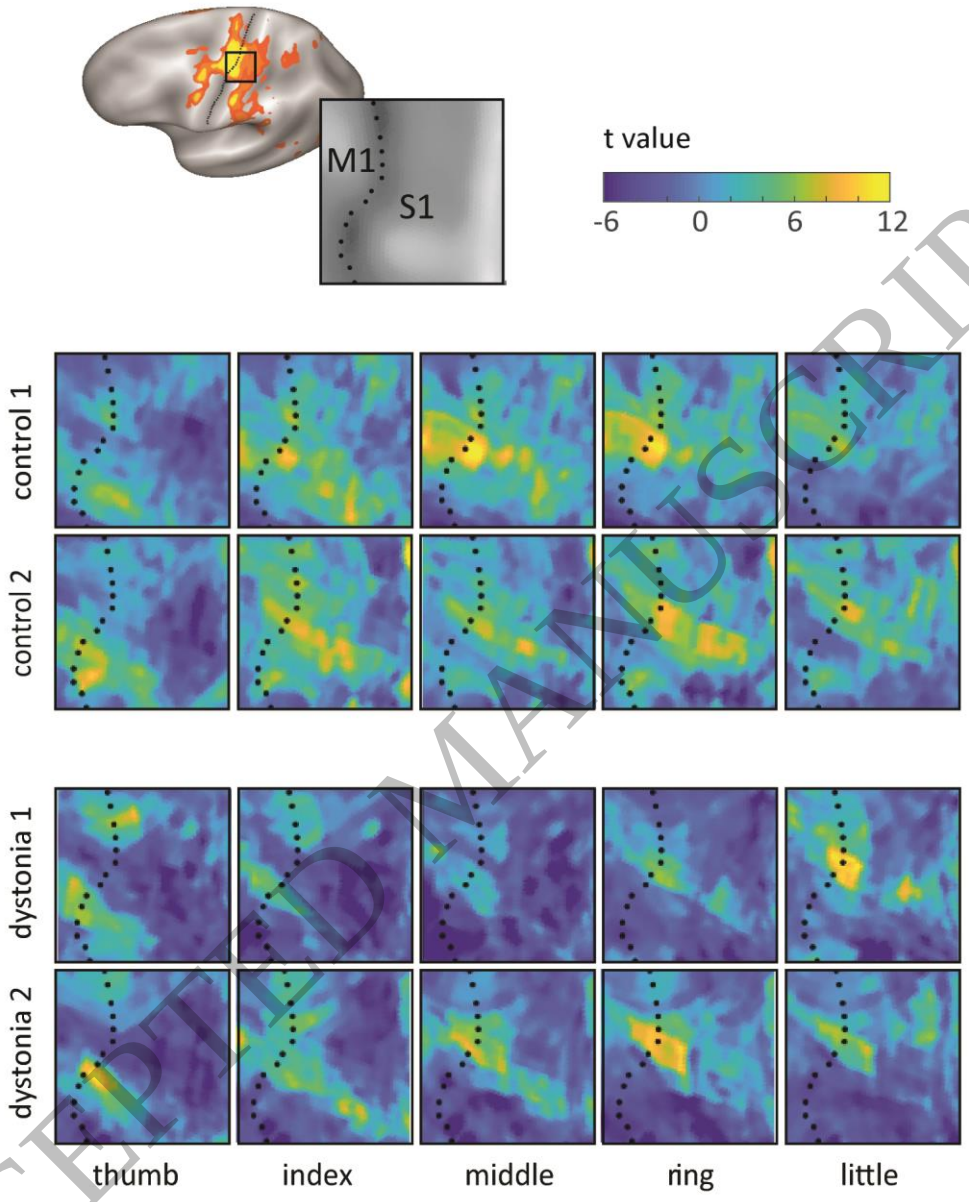

Figure 2
135x170 mm (5.2 x DPI)

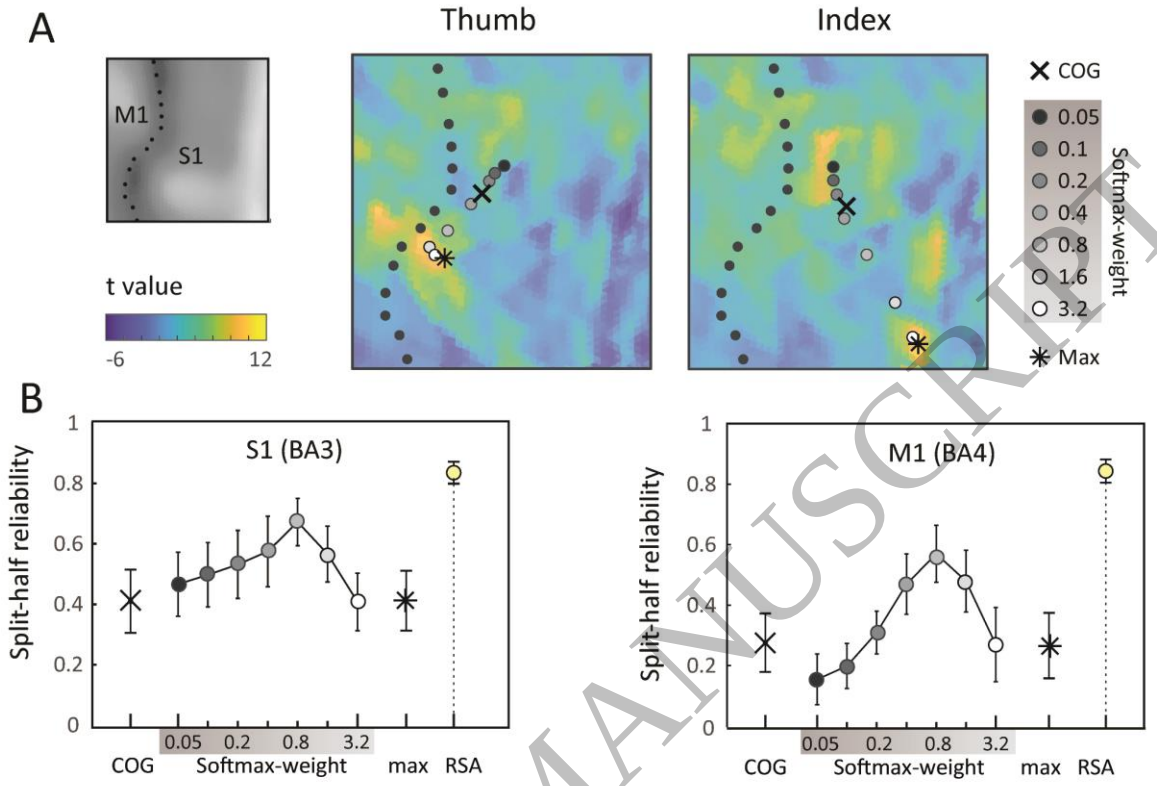

Figure 3
159x111 mm (5.2 x DPI)

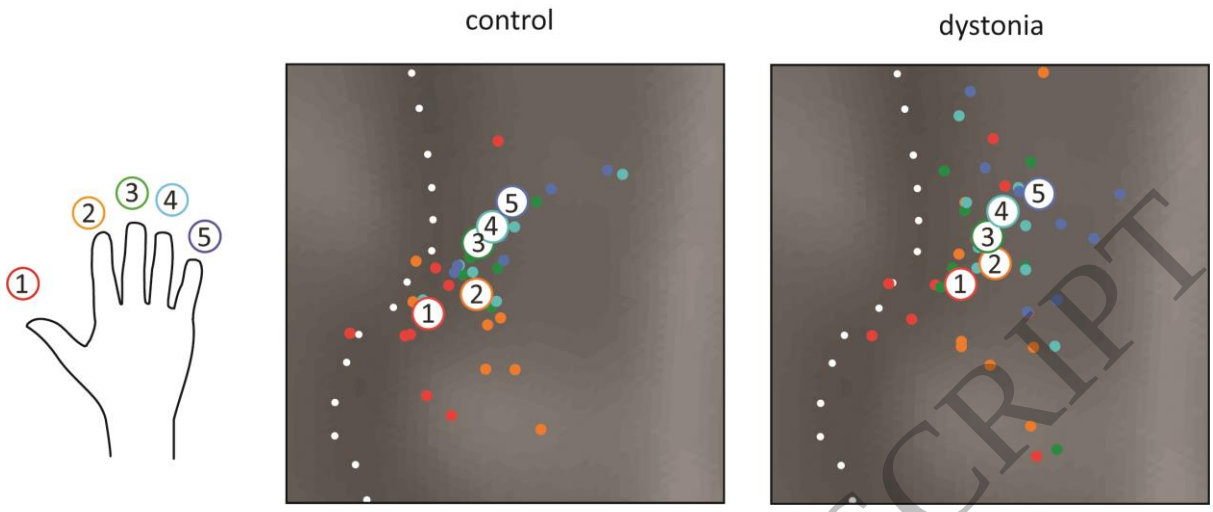

Figure 4
159x66 mm (5.2 x DPI)

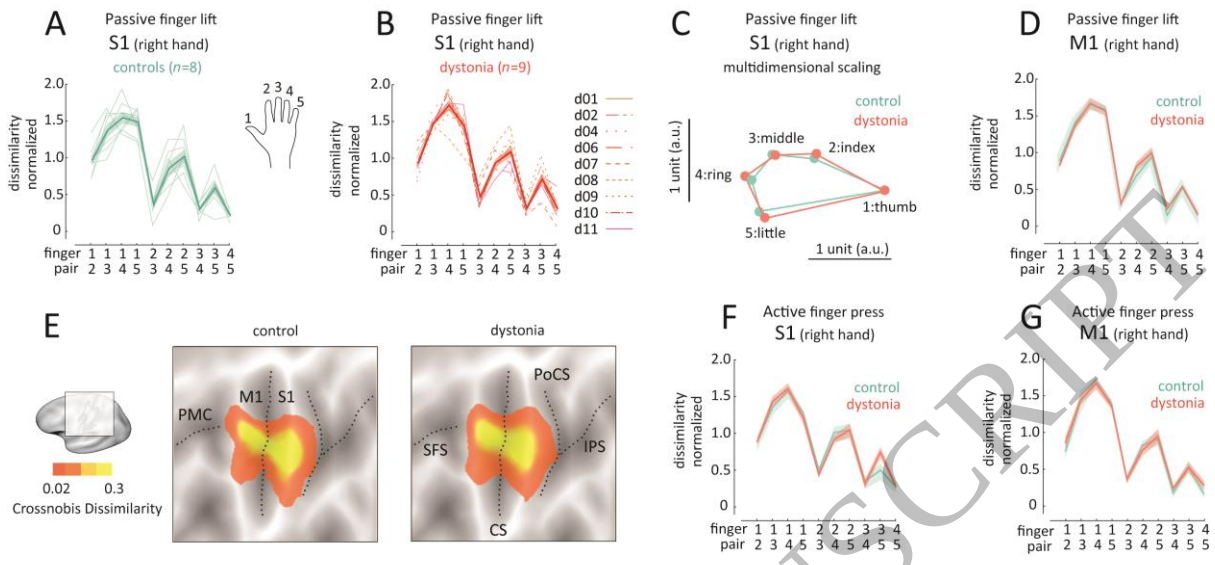

Figure 5
159x73 mm (5.2 x DPI)

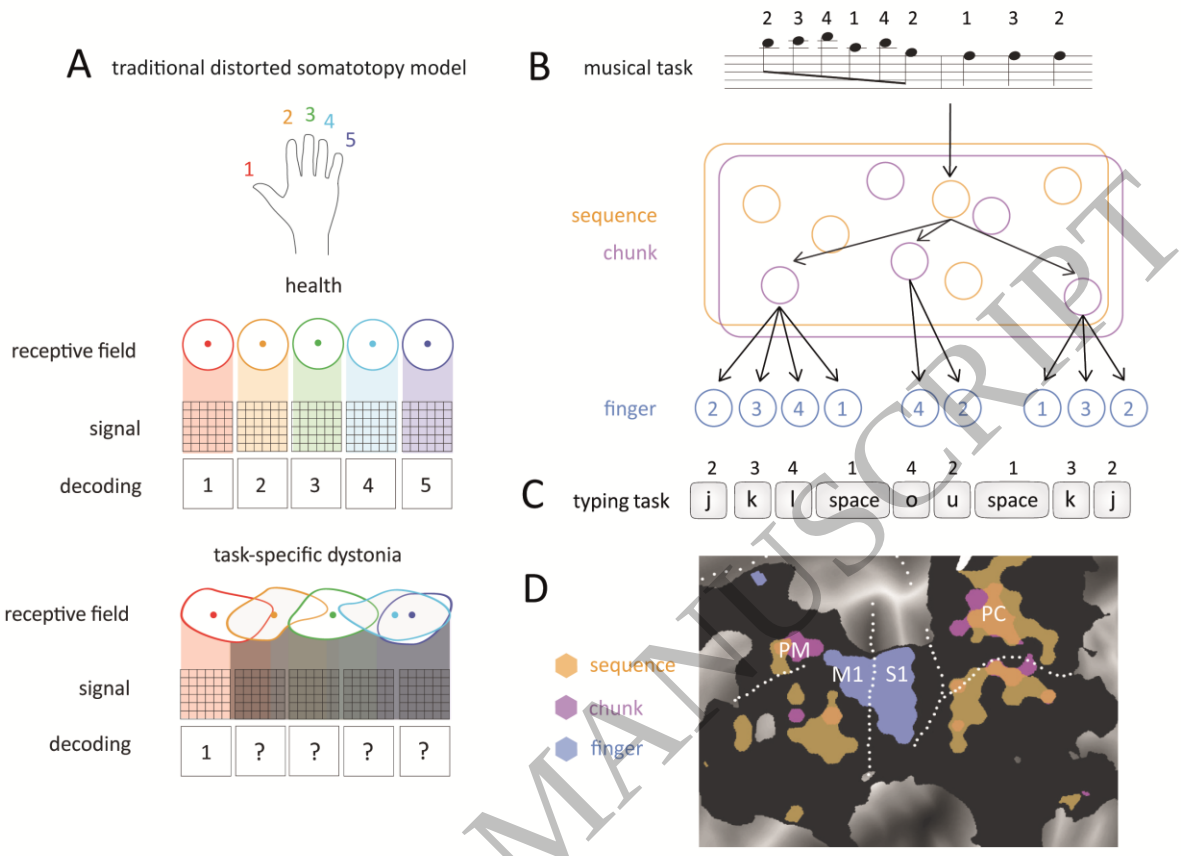

Figure 6
159x118 mm (5.2 x DPI)